Research Square

Preprints are preliminary reports that have not undergone peer review.
They should not be considered conclusive, used to inform clinical practice,
or referenced by the media as validated information.

Bioactivity of Recombinantly Expressed Human Serglycin Under Different Glycemic Conditions

Shang-Wun Jhang
Changhua Christian Hospital
Ya-Ning Chang
National Chung-Hsing University
Chiu-Chen Huang
Asia University
Yu-Ting Yan
Academia Sinica
Bill Cheng
bcheng@dragon.nchu.edu.tw

National Chung-Hsing University

Research Article

Keywords: Serglycin, Glycosaminoglycans, Recombinant proteins, Wound Healing, Re-epithelization

Posted Date: February 26th, 2026

DOI: https://doi.org/10.21203/rs.3.rs-8846113/v1

License: This work is licensed under a Creative Commons Attribution 4.0 International License.
Read Full License

Additional Declarations: No competing interests reported.

Abstract

Background

Human platelet lysate (hPL) is clinically used for chronic wound treatment, yet therapeutic responses remain variable due to the undefined roles of individual platelet-derived components. Serglycin (SRGN) is abundant in platelet granules, but its function in diabetic wound repair is poorly understood. This study investigated the bioactivity of recombinant human serglycin (rhSRGN) in an in vitro model of diabetic re-epithelialization.

Results

SRGN cDNA was amplified from THP-1-derived mRNA, cloned into an expression vector, and transfected into HEK293T cells for recombinant protein production. Secreted rhSRGN was purified from conditioned media via immobilized metal affinity chromatography using a C-terminal 6×His tag. Western blotting confirmed that rhSRGN carried multiple glycosaminoglycan chains, including heparan sulfate, chondroitin sulfate, and dermatan sulfate. Functionally, rhSRGN (10 ng/mL) significantly enhanced keratinocyte migration under hyperglycemic conditions in a wound closure assay.

Conclusions

Recombinant serglycin promotes keratinocyte migration in a hyperglycemic microenvironment, supporting its potential as a defined platelet-derived biologic for bioengineered therapies targeting diabetic wound healing.

Introduction

Diabetic wounds remain a major clinical challenge worldwide. In Taiwan, where the prevalence of diabetes mellitus (DM) is high, it has been estimated that approximately 15% of patients with DM develop diabetic wounds[1]. This condition is characterized by impaired wound healing, which increases the risk of infection, limb amputation, and other severe complications. Beyond the substantial burden on patient quality of life, diabetic wounds also impose high socioeconomic costs on healthcare systems[2].

Clinically, re-epithelialization is considered one of the most critical phases of wound repair, as it restores the epidermal barrier and prevents microbial invasion. However, in diabetic wounds, this process is often delayed or incomplete due to multiple pathological factors, including persistent hyperglycemia, chronic inflammation, impaired angiogenesis, reduced growth factor availability, and dysfunctional keratinocyte migration[3]. Consequently, promoting re-epithelialization has become a central objective in the development of diabetic wound therapies.

Although an enormous number of studies have been published on diabetic wound healing, and several advanced wound care products are currently available in clinical practice, therapeutic outcomes remain inconsistent. Many existing treatments provide only partial benefits, and a substantial proportion of patients still experience non-healing or recurrent ulcers[4]. This variability reflects the complex and multifactorial nature of diabetic wounds, as well as the limitations of current interventions in effectively addressing the impaired cellular responses required for tissue regeneration. Therefore, there remains a continuous and urgent need to develop more effective and mechanistically informed therapeutics that can reliably promote re-epithelialization in diabetic wound healing.

Human platelet lysate (hPL), a protein-rich solution prepared from platelet lysis, has been widely used clinically to treat chronic and diabetic wounds, as platelets contain numerous bioactive molecules that contribute to tissue repair, including growth factors, cytokines, and extracellular matrix–modulating proteins. hPL therapy has shown promising outcomes in some patients, yet clinical reports have also indicated limited efficacy in others[5]. Importantly, hPL is a complex mixture, and the biological functions of many of its individual components remain insufficiently characterized[6]. This incomplete understanding hinders the optimization and standardization of platelet-derived therapies and may contribute to variable patient responses.

Serglycin (SRGN) is a proteoglycan abundantly present in platelet granules[7]. A defining feature of SRGN is the presence of glycosaminoglycan (GAG) chains attached to its protein core, which enable it to bind and transport multiple growth factors and inflammatory mediators[8]. Upon platelet activation, these SRGN-associated factors can be released into the wound microenvironment[9], potentially influencing key processes such as keratinocyte migration, inflammation, and extracellular matrix remodeling. Despite its abundance in platelets and presence in hPL, the functional role of SRGN in chronic wound repair, particularly under diabetic conditions, remains largely unknown (Fig. 1).

Given the growing clinical interest in platelet-derived biomaterials, elucidating the contribution of specific components such as SRGN is important for improving the mechanistic understanding of hPL-based therapies. Furthermore, identifying previously unrecognized bioactive factors within hPL may support the development of more targeted, reproducible, and effective therapeutic strategies for diabetic wound healing.

Thus, this study aimed to evaluate the bioactivity of SRGN using an *in vitro* model that mimics re-epithelialization in diabetic wounds. Because SRGN is difficult and costly to purify from natural sources, recombinant DNA technology was employed to produce recombinant human SRGN (rhSRGN). In addition, the GAG composition of rhSRGN was characterized, and its bioactivity in promoting keratinocyte migration under hyperglycemic conditions was investigated.

Materials & Methods

Recombinant Vector Construction

Total RNA was extracted from human THP-1 monocytes (ATCC, Cat# TIB-202) using the TRIzol extraction method. After RNA isolation, first-strand cDNA was synthesized using the ProtoScript First Strand cDNA Synthesis Kit (NEB, Cat# E6300S). Following synthesis according to the manufacturer's protocol, the resulting cDNA was subjected to PCR amplification to obtain the SRGN cDNA sequence.

PCR amplification was performed using the Promega PCR Master Mix (Promega, Cat# M7502). Reaction mixtures were prepared according to the manufacturer's instructions, with primers targeting the serglycin (SRGN) gene of interest (GOI) added as follows: forward primer, 5'-ATGGATCCACCATGATGCAGAAGCTACTCAAATGC-3'; and reverse primer, 5'-ATGAATTCTAACATAAAATCCTCTTCTAATCCATGT-3'. The SRGN cDNA fragment was amplified using a PCR thermal cycler (Turbocycler Lite, Blue-Ray Biotech Corp., Taiwan), yielding a 477-bp product (**Supplementary Fig. 1**).

The forward primer contained a *Pme*I restriction site, while the reverse primer contained a *Bam*HI restriction site. This design enabled the SRGN cDNA to incorporate a *PmeI* site at its 5' end and a *Bam*HI site at its 3' end. The SRGN cDNA was digested with the restriction enzymes *PmeI* (NEB, Cat. # R0560S) and *Bam*HI (NEB, Cat. # R0136S), and subsequently cloned into the expression vector pcDNA4/myc-HisA (a gift from Yu-Ting Yan, Academia Sinica) using T4 DNA ligase (NEB, Cat. # M0202). The resulting recombinant plasmid was designated as pcDNA4/SRGN-HisA.

Recombinant Vector Expressions and Mammalian Cell Transfection

The pcDNA4/SRGN-HisA vector was transformed into *E.coli* JM109 competent cells for amplification of the recombinant plasmid. Subsequently, the transformed bacteria were plated onto agar plates containing ampicillin for selection. Cells that did not carry the plasmid were unable to survive, whereas plasmid-containing colonies grew under antibiotic pressure. Surviving colonies were picked and cultured in LB broth at 37°C. Plasmid DNA was then extracted in large quantities using the GeneDireX Plasmid MiniPREP Kit (Cat. # NA005-0100). Successful cloning of the SRGN cDNA insert into the expression vector was confirmed by agarose gel electrophoresis (1% agarose), and the sequence was further verified by DNA sequencing.

For recombinant human serglycin (rhSRGN) expression, pcDNA4/SRGN-HisA was transfected into HEK293T cells (ATCC, Cat# CRL-3216). Cells were cultured in high-glucose DMEM (Gibco, Cat. # 11965092) supplemented with 10% fetal bovine serum (FBS) and 1% penicillin–streptomycin (P/S) until reaching approximately 80% confluence. Transfection complexes were prepared according to the manufacturer's protocol. Briefly, Lipofectamine 3000 reagent (Thermo Fisher Scientific) was diluted in Opti-MEM medium (Thermo Fisher, Cat. # 31985062). In parallel, plasmid DNA was diluted in Opti-MEM and mixed with P3000 reagent. The diluted DNA solution was then combined with diluted Lipofectamine 3000 at a 1:1 ratio to form DNA–lipid complexes.

The complexes were added to HEK293T cells and incubated for 10–15 min at room temperature. Cells were then cultured overnight at 37°C. Transfected cells were selected using 400 μg/mL zeocin (Thermo Fisher, Cat. # R25001). The resulting stable cell line was designated as HEK293T-SRGN.

Purification of Recombinant Human Serglycin

Recombinant human serglycin (rhSRGN) secreted into the conditioned medium of HEK293T-SRGN cells was purified according to a previously published method[10]. Briefly, conditioned medium containing rhSRGN was loaded onto a nickel-chelate affinity column (Merck, Cat. # GE17-5248-02) and allowed to circulate through the column overnight at 4°C. The following day, unbound proteins were removed by washing with at least 10 column volumes of binding buffer (0.5 M NaCl, 0.04 M imidazole, 0.02 M sodium phosphate, pH 7.4). Bound proteins were then eluted using elution buffer (0.5 M NaCl, 0.5 M imidazole, 0.02 M sodium phosphate, pH 7.4).

The eluate was collected and dialyzed against saline buffers. The rhSRGN-containing solution was further enriched by anion exchange chromatography using a diethylaminoethyl (DEAE) column (Merck, Cat. # GE17-5154-01). The DEAE column was equilibrated with running buffer (250 mM NaCl, 20 mM Tris, 10 mM EDTA, pH 7.5) before sample loading. After loading, the column was washed with 10 column volumes of running buffer, and rhSRGN was eluted with elution buffer (1 M NaCl, 20 mM Tris, 10 mM EDTA, pH 7.5). The eluted protein was subsequently concentrated by dialysis. Finally, rhSRGN concentration was quantified using a human serglycin ELISA kit (ABclonal, Cat. # RK09141) according to the manufacturer's instructions.

Cell culture.

Human keratinocyte HaCaT cells (Cat. # 300493, CLS) were cultured under normoglycemic conditions in low-glucose DMEM (Cat. # 11885084, Gibco) supplemented with 1% fetal bovine serum (FBS; Cat. # 10437028, Gibco) and 1% penicillin–streptomycin (P/S; Cat. # 15140122, Gibco). For hyperglycemic conditions, HaCaT cells were cultured in high-glucose DMEM (Cat. # 11965092, Gibco) containing 1% FBS and 1% P/S.

In vitro wound healing assay.

The Ibidi stage top incubation system (Cat. # 10720, Ibidi) was used for live-cell imaging of HaCaT migration. Cells were first seeded into a 2-well culture insert (Cat. # 80209, Ibidi) in low-glucose medium and cultured overnight. The following day, the culture insert was removed, and HaCaT cells were imaged under either low- or high-glucose conditions, with or without 10 ng/mL rhSRGN.

To silence CD44 expression in HaCaT cells, cells were transfected with CD44 siRNA (Thermo Fisher Scientific, Cat. # 4390771). Results were compared with those from cells transfected with a negative control siRNA (Thermo Fisher Scientific, Cat. # 4390843). Either CD44 siRNA or negative control siRNA was delivered into cells using Lipofectamine RNAiMAX (Thermo Fisher Scientific, Cat. # 13778030).

Cells were seeded into the 2-well insert at a density of 4×10^5 cells/mL. The next day, the transfection mixture was prepared by diluting Lipofectamine RNAiMAX reagent in Opti-MEM. In parallel, siRNA was diluted in Opti-MEM. The diluted Lipofectamine and siRNA solutions were then combined and incubated at room temperature for 20 min to allow complex formation. The complexes were subsequently added to the cells in the 2-well insert. After transfection, the insert was removed, and the cells were placed in the Ibidi Stage Top Incubator for live-cell imaging experiments.

Dodecyl Sulfate Polyacrylamide Electrophoresis (SDS-PAGE) and Western Blotting. 4%–12% SDS–polyacrylamide gels (Cat. # HC2040, Thermo Fisher Scientific) were prepared according to the manufacturer's protocol using the Mini-PROTEAN® Tetra Handcast System (Cat. # 1658000FC, Bio-Rad). Samples were electrophoresed at 100 V at room temperature until the dye front reached the bottom of the gel. Proteins were subsequently transferred onto a polyvinylidene fluoride (PVDF) membrane (0.45 µm; Cat. # IPVH00010, Merck Millipore).

After blocking overnight at 4°C, membranes were incubated with primary antibodies at 4°C with gentle shaking overnight. The membranes were then washed with 0.1% TBST and incubated with secondary antibodies for 1 h at room temperature with shaking. Following additional washes with 0.1% TBST, immunoreactive signals were detected using ECL Plus reagent (Cat. # WBKLS0500, Merck Millipore).

Human platelet lysates were bought from a commercial supplier (Mill Creek, Cat # PLTGold). Anti-human serglycin antibody (Cat. # A6951) was purchased from ABclonal. Anti-chondroitin sulfate antibody (Cat. # SAB4200696), anti-heparan sulfate antibody (Cat. # MAB2040), and anti-dermatan sulfate antibody (Cat. # MABT819) were purchased from Merck Millipore. Anti-human TGFβ1 (Cat. # GTX130023), anti-human ERK1/2 (Cat. # GTX134462), anti-phospho-p38 MAPK (Cat. # GTX110720), anti-phospho-AKT (Ser473) (Cat. # GTX128414), and anti-human β-actin (Cat. # GTX109639) were purchased from GeneTex. Peroxidase AffiniPure goat anti-rabbit IgG (Cat. # 111-035-144) and Peroxidase AffiniPure goat anti-mouse IgG (Cat. # 115-035-003) were purchased from Jackson ImmunoResearch Laboratories.

Statistical analysis.

One-way analysis of variance test and then Tukey post-hoc test were used to compare the statistical significance between treatments under test conditions. A *P* value of less than 0.05 was considered significant.

Results

Construction of pcDNA4/SRGN-HisA Vectors

Monocytes share a common hematopoietic lineage with platelets[11]; therefore, total RNA extracted from human THP-1 monocytes was used as the template for amplification of the serglycin (SRGN) gene of interest (GOI, **Supplementary Fig. 1**). After successful amplification, the SRGN cDNA fragment was cloned into the pcDNA4/myc-HisA expression vector using *PmeI* and *BamHI* restriction digestion. The

resulting recombinant plasmid was subsequently transformed into *E. coli* JM109 for vector amplification.

Prior to transfection into HEK293T cells for recombinant protein production, successful insertion of the SRGN GOI into the pcDNA4/HisA vector was confirmed by agarose gel electrophoresis (Fig. 2a). The undigested pcDNA4/HisA vector appeared as a high–molecular–weight band (> 10,000 bp), likely due to plasmid supercoiling and aggregation. After linearization with *Pme*I and *Bam*HI, the expected vector size was observed at approximately 5,000 bp.

In contrast, the undigested recombinant pcDNA4/SRGN-HisA plasmid displayed two bands, one above 10,000 bp and another around 6,000 bp. Importantly, double digestion of pcDNA4/SRGN-HisA produced two distinct bands: one at approximately 5,000 bp corresponding to the vector backbone, and another at approximately 500 bp corresponding to the inserted SRGN GOI. These results confirm that the recombinant expression vector was successfully constructed.

Mammalian Expressions of rhSRGN

The rhSRGN cDNA construct included its native signal peptide sequence, enabling the recombinant protein to be secreted into the conditioned medium by HEK293T-SRGN cells[12]. In addition, rhSRGN carried a C-terminal 6×His tag, which allowed purification from the conditioned medium using a nickel-chelate affinity column. Furthermore, the negatively charged glycosaminoglycan (GAG) chains attached to the serglycin core protein enabled additional purification by anion exchange chromatography[13]. The amount of rhSRGN purified from each batch was quantified, and the differences among batches were negligible (**Supplementary Table 1**).

The yield of secreted rhSRGN in the conditioned medium on each day post-transfection was also quantified (**Supplementary Fig. 2**). Four independent batches of conditioned medium were analyzed, and only small, non-significant variations in rhSRGN concentration were observed among the batches. Batch A consistently produced the highest yield of rhSRGN throughout the 6-day culture period, followed by Batch D, Batch B, and Batch C. These differences occurred despite the use of the same transfection protocol to establish clones in all four batches. Similar variability has been reported in other recombinant protein production studies, as lipofection-based transfection cannot precisely control the number of plasmid copies delivered into each cell[14]. Therefore, it is likely that HEK293T-SRGN cells in Batches B–D incorporated fewer pcDNA4/SRGN-HisA vectors during the initial transfection process compared with Batch A, resulting in lower rhSRGN production in those batches.

Characterizations of rhSRGN

To determine whether the rhSRGN structurally resembled native serglycin (SRGN), rhSRGN purified from all four batches was characterized by Western blotting and compared with endogenous SRGN detected in THP-1 cell lysate (**Supplementary Fig. 3**). When probed with anti-human serglycin antibodies, SRGN in

THP-1 lysate appeared as multiple distinct bands at various molecular weights, accompanied by a faint background smear. In contrast, no immunoreactivity was observed in the lane loaded with HEK293T cell lysate. Notably, rhSRGN from all four batches exhibited similar banding patterns to one another and closely resembled SRGN detected in THP-1 lysate. However, the smear pattern in the rhSRGN lanes was more pronounced than that observed in THP-1 lysate, suggesting that rhSRGN may contain a higher degree of glycosylation and/or more extensively decorated GAG chains[15].

rhSRGN purified from Batch A was used for subsequent experiments. To further confirm that rhSRGN exhibited structural features similar to native SRGN, additional Western blot analyses were performed to examine the GAG composition of rhSRGN. The results were compared with SRGN present in commercially available human platelet lysate (hPL) (Fig. 2b**)**. In these experiments, protein samples were heated at 60°C for 20 min before electrophoresis to improve epitope accessibility for anti-GAG antibodies.

When probed with anti-SRGN antibodies, rhSRGN displayed a blotting pattern similar to SRGN in THP-1 lysate, with strong signals ranging from approximately 25 kDa to 180 kDa. In addition, a band at ~ 15 kDa was detected in both samples, likely corresponding to the serglycin core protein. In contrast, hPL exhibited a broader smear pattern from ~ 35 kDa to ~ 180 kDa, suggesting that SRGN in hPL may carry a lower degree of GAG glycosylation compared with rhSRGN. Consistent with previous results[16], HEK293T lysate showed no reactivity with anti-SRGN antibodies.

Since chondroitin sulfate (CS) is the predominant GAG type associated with SRGN in monocytes and hPL[17], anti-CS antibodies were used to assess CS decoration on rhSRGN. Anti-CS probing produced smear patterns in THP-1 lysate, hPL, and rhSRGN, although the molecular weight distributions differed among the samples. Strong CS signals were observed in THP-1 lysate between ~ 35 kDa and ~ 60 kDa. In hPL, distinct bands were detected at ~ 140 kDa, ~ 60 kDa, and ~ 35 kDa, with a faint smear between these regions. rhSRGN exhibited anti-CS reactivity from ~ 35 kDa to ~ 140 kDa, indicating a distinct CS modification profile compared with THP-1 SRGN and hPL-derived SRGN. As expected, HEK293T lysate showed no anti-CS reactivity.

Probing with anti-dermatan sulfate (DS) antibodies produced a smear pattern from ~ 35 kDa to ~ 140 kDa in both THP-1 lysate and rhSRGN. In hPL, DS reactivity appeared as a smear extending from ~ 60 kDa to ~ 180 kDa, along with a distinct band at ~ 35 kDa and a faint smear between ~ 35 kDa and ~ 60 kDa. Similarly, anti-heparan sulfate (HS) antibodies detected strong signals in THP-1 lysate spanning ~ 15 kDa to ~ 100 kDa, whereas rhSRGN showed strong HS reactivity from ~ 35 kDa to ~ 140 kDa. In hPL, HS-associated signals were observed from ~ 60 kDa to ~ 180 kDa, together with a distinct band at ~ 35 kDa.

Collectively, these results confirm that rhSRGN was successfully expressed and secreted by HEK293T-SRGN cells transfected with pcDNA4/SRGN-HisA. rhSRGN reacted strongly with anti-SRGN antibodies and exhibited banding patterns comparable to SRGN detected in THP-1 lysate and hPL. Furthermore, rhSRGN was shown to be decorated with multiple GAG types, including CS, DS, and HS. Although the

precise arrangement of these GAG chains on individual rhSRGN molecules remains unclear, the detection of multiple GAG species suggests that rhSRGN exists as a heterogeneous population with variable GAG modifications (Fig. 2c).

Cell Proliferation and Viability Analyses

Before performing functional assays with rhSRGN, its effects on keratinocyte proliferation and viability were evaluated. Human keratinocytes (HaCaT) were cultured in either normal-glucose (**NG**, 5.5 mM) or high-glucose (**HG**, 25 mM) medium, with or without 10 ng/mL rhSRGN, and cell morphology was examined by light microscopy (Fig. 3a). A concentration of 10 ng/mL was selected for subsequent cell-based assays, as it is commonly used to assess the bioactivity of purified recombinant proteins[18]. To minimize potential interference from serum components and preserve rhSRGN bioactivity, all HaCaT assays were performed in medium containing 1% FBS.

Distinct morphological differences were observed between HaCaT cells cultured under NG and HG conditions. At Days 1 and 3, cells cultured in HG exhibited smaller colony sizes and fewer colonies compared with those cultured in NG. By Day 5, high cell confluence was observed in both glucose conditions. Interestingly, supplementation with rhSRGN resulted in the formation of smaller colonies in both NG- and HG-treated groups.

Over the 5-day culture period, HaCaT cells cultured in NG medium exhibited the highest proliferation rate among all groups (Fig. 3b). Glucose concentration significantly affected cell proliferation, as HaCaT cells cultured in HG displayed significantly reduced cell numbers compared with those cultured in NG. Notably, the addition of rhSRGN in NG medium led to a significant decrease in cell number, suggesting that rhSRGN may inhibit keratinocyte proliferation under normoglycemic conditions. In contrast, rhSRGN supplementation in HG medium did not significantly affect HaCaT proliferation throughout the culture period.

Cell viability was also assessed over the 5-day culture period (Fig. 3c). Although glucose concentration significantly influenced proliferation, no corresponding differences were observed in cell viability. No significant differences in viability were detected among the four experimental groups, indicating that elevated glucose levels did not induce substantial cytotoxicity. Importantly, rhSRGN treatment did not result in increased cell death under either NG or HG conditions.

Keratinocyte migration with or without the rhSRGN

To investigate the therapeutic potential of rhSRGN in a chronic wound setting, an in vitro wound-healing model that mimics re-epithelialization under hyperglycemic conditions was established (Fig. 4a). Human keratinocytes (HaCaT) were cultured in a 2-well insert system, in which the gap between the cell monolayers represented the “wound.” Cell migration toward the center of the gap, reflecting wound closure, was monitored using an Ibidi Stage Top Incubator coupled with a live-cell imaging system, followed by Western blot analysis.

Under normoglycemic (NG) conditions, HaCaT cells effectively closed the gap after 20 h of incubation. In contrast, the gap remained visible in HaCaT cultures maintained in high-glucose (HG) medium after the same period. Interestingly, rhSRGN supplementation reduced the ability of cells to close the gap under NG conditions, whereas the same treatment enhanced cell migration under HG conditions.

Quantitatively, no significant differences in migration rates were observed among the four groups during the first 4 h of the assay (Fig. 4b). However, at 12 h, HaCaT cells cultured in HG medium supplemented with rhSRGN migrated significantly faster than those in the other three groups. This enhanced migration persisted at 16 h. As expected, HaCaT cells cultured in NG medium migrated significantly faster than those cultured in HG medium, as well as those cultured in NG medium supplemented with rhSRGN. By 20 h, no significant difference was observed between cells cultured in NG medium and those cultured in HG medium with rhSRGN, although a smaller residual gap was still present in the latter group.

To further analyze the effects of glucose concentration and rhSRGN treatment on keratinocyte migration, cell lysates were collected at the end of the migration experiments and subjected to Western blot analysis. The expression of four migration-associated protein markers was examined (Fig. 5a), and protein levels were normalized to β-actin expression (Fig. 5b). Phosphorylated p38 MAPK (p-p38 MAPK), phosphorylated Akt (p-Akt), phosphorylated Erk1/2 (p-Erk1/2), and TGFβ1 are known to play important roles in cell migration[19].

HaCaT cells cultured under NG conditions exhibited significantly higher expression levels of all four proteins compared with those cultured in HG medium. In NG medium supplemented with rhSRGN, p-p38 MAPK expression was slightly reduced compared with NG alone, although this difference was not statistically significant. In contrast, p-Akt, p-Erk1/2, and TGFβ1 levels were significantly higher in NG cultures treated with rhSRGN compared with untreated NG controls. Notably, under HG conditions, rhSRGN supplementation resulted in significantly increased expression of all four migration-related markers compared with HG medium alone.

Keratinocyte migration following CD44 silencing in the presence or absence of rhSRGN

Previous studies have reported that serglycin can promote cancer cell migration through interactions with CD44 membrane receptors[20]. Therefore, we investigated whether the bioactivity of rhSRGN in HaCaT keratinocytes would be attenuated following CD44 silencing. HaCaT cells cultured in the 2-well insert system were transfected with CD44 siRNA and incubated overnight at 37°C. To confirm the specificity of CD44 knockdown, a parallel culture of HaCaT cells was transfected with a negative control siRNA, consisting of RNA sequences that do not target any known mRNA.

On the following day, cells transfected with either negative control siRNA or CD44 siRNA were subjected to an in vitro wound-healing assay overnight. Cell lysates were then harvested, and CD44 expression levels were examined (**Supplementary Fig. 4**).

Western blot analysis using anti-human CD44 antibodies revealed that HaCaT cells transfected with CD44 siRNA exhibited minimal CD44 expression, whereas strong CD44 expression was detected in cells transfected with negative control siRNA. These results confirmed that CD44 siRNA effectively silenced CD44 expression in HaCaT cells. To further demonstrate the specificity of the knockdown, the expression of another membrane protein, syndecan-1, was assessed. Syndecan-1 expression remained strong and comparable between cells transfected with negative control siRNA and those transfected with CD44 siRNA. Collectively, these findings indicate that CD44 silencing was specific and did not broadly affect membrane protein expression.

After successful validation of CD44 knockdown under normoglycemic conditions, HaCaT cells were subjected to an in vitro wound-healing assay to evaluate the effects of rhSRGN treatment (Fig. 6a). Under normoglycemia, CD44-silenced HaCaT cells migrated more slowly than cells transfected with negative control siRNA. Notably, the motility of CD44-silenced HaCaT cells in NG medium increased in the presence of rhSRGN. In contrast, CD44-silenced HaCaT cells cultured in HG medium exhibited migration rates similar to those of negative control cells. The addition of rhSRGN to HG medium also appeared to enhance the migration of CD44-silenced HaCaT cells after 20 h of incubation.

To determine whether the differences observed in the time-lapse images were statistically significant, the experiments were repeated three times for each group, followed by quantitative analysis (Fig. 6b). During the first 4 h of the assay, HaCaT cells cultured in NG medium displayed significantly higher migration rates than all other groups. At 12, 16, and 20 h, HaCaT cells cultured in NG medium continued to migrate significantly faster than CD44-silenced HaCaT cells under NG conditions. Migration was also significantly enhanced when rhSRGN was added to CD44-silenced HaCaT cells in NG medium, indicating that rhSRGN partially restored migration despite CD44 knockdown.

In contrast, no significant differences were observed among the HG groups until 20 h. At 20 h, rhSRGN significantly enhanced the migration rate of CD44-silenced HaCaT cells cultured in HG medium compared with untreated CD44-silenced cells. The untreated CD44-silenced cells in HG medium also migrated significantly more slowly than HaCaT cells cultured in HG medium without knockdown. However, the difference between HaCaT cells cultured in HG medium and CD44-silenced HaCaT cells cultured in HG medium with rhSRGN was not statistically significant.

To further evaluate the impact of CD44 silencing on migration-related signaling under different glucose conditions, cell lysates were collected at the end of the wound-healing assay and analyzed by Western blotting. The expression levels of p-p38 MAPK, p-Akt, p-Erk1/2, and TGFβ1 were examined (Fig. 7a). In the absence of rhSRGN, these four markers were barely detectable in migrating HaCaT cells under either NG or HG conditions. In contrast, rhSRGN treatment significantly elevated the expression of all four proteins in cells cultured in both glucose conditions (Fig. 7b).

Collectively, these results suggest that CD44 silencing significantly attenuated the ability of rhSRGN to promote HaCaT migration under hyperglycemic conditions. Meanwhile, CD44 knockdown reversed the

inhibitory effect of rhSRGN under normoglycemia, as migration rates were enhanced compared with non-silenced HaCaT cells treated with rhSRGN in NG medium.

Discussion

Human platelet lysates (hPL) have been widely explored as therapeutic formulations for chronic diabetic wounds due to their rich composition of growth factors, cytokines, and extracellular matrix–associated proteins. However, clinical outcomes remain variable, in part because hPL is intrinsically heterogeneous and subject to donor-to-donor variability, differences in preparation protocols, and risks of contamination during processing[21]. These challenges highlight an ongoing need in biological engineering to move toward defined, standardized, and scalable platelet-derived biologics, rather than relying on complex and poorly controlled mixtures[22].

Serglycin is a proteoglycan known to regulate the storage and extracellular activity of multiple growth factors in platelet granules, including VEGF and PDGF[23]. Historically, serglycin has been characterized primarily as a molecular carrier that facilitates intracellular packaging and extracellular delivery of signaling proteins. In the absence of serglycin, growth factor secretion and activity can be impaired, which may compromise the wound-healing cascade [24]. However, whether serglycin itself possesses independent therapeutic activity after dissociation from its binding partners has remained unclear. In this study, recombinant human serglycin (rhSRGN) was produced using recombinant DNA technology and evaluated as a defined bioactive component that modulates keratinocyte behavior under hyperglycemic conditions. This work supports the broader concept that engineered platelet-derived proteoglycans may represent an emerging class of biologics for chronic wound repair.

Engineering and Structural Characterization of rhSRGN

Western blot analysis confirmed that rhSRGN production resulted from the successful transfection of pcDNA4/SRGN-HisA into HEK293T cells, as serglycin was not detected in non-transfected controls. Importantly, proteoglycans such as serglycin exhibit substantial heterogeneity in GAG chain length and sulfation, which typically manifests as a smear pattern on Western blots[25]. The broad molecular weight distribution observed for rhSRGN and THP-1–derived serglycin suggests variable glycosylation states, whereas the narrower distribution observed in hPL may reflect a less diverse serglycin population within platelet-derived preparations.

A ~ 15 kDa band detected in THP-1 lysates and rhSRGN samples likely corresponds to the serglycin core protein. Although the theoretical molecular weight is ~ 18 kDa, reported values vary widely (~ 26 kDa to ~ 8kDa) due to post-translational modifications[7]. The absence of this band in hPL may be attributable to platelet biology, as platelets lack transcriptional machinery and acquire serglycin from megakaryocytes during thrombopoiesis rather than synthesizing it directly[26].

Notably, rhSRGN was found to carry CS, DS, and HS chains. In native monocytes and platelets, serglycin is typically decorated with CS and DS[17], whereas HS signals in THP-1 lysates may partly originate from

syndecan-1, an HS proteoglycan expressed in monocytes and platelets[27]. Recombinant expression systems such as HEK293T are known to generate proteoglycans with altered or expanded GAG profiles compared with native cells[16]. Therefore, rhSRGN likely represents a heterogeneous population with variable GAG composition and charge density. Since GAG identity strongly influences binding interactions with growth factors (HS > CS > DS in negative charge density), structural heterogeneity may directly impact biological function[28]. From a bioengineering standpoint, these findings emphasize that glycoengineering and molecular standardization will be critical considerations in the future development of serglycin-based therapeutics.

Functional Effects Under Hyperglycemic Wound Conditions

The therapeutic value of the rhSRGN as a bioactive was demonstrated in an *in vitro* assay that studied keratinocyte migration under hyperglycemia. Although the *in vitro* model was a 2D culture, the model had been implicated by others as an excellent assay in evaluating re-epithelization under various conditions[29]. The assay clearly revealed that when HaCaT cultured in NG media, which contained a similar glucose level as the blood glucose level (5.5mM) in a healthy person[30], the cells were able to migrate efficiently towards the center, indicated efficient wound closure rate. In contrast, HaCaT cultured in the HG media, which contained five times the glucose level (25 mM) as the NG media, displayed a significantly slower migration rate. Previous studies have indicated that HaCaT cultured in media containing 25 mM glucose displayed similar pathological responses as keratinocytes in a diabetic wound[31].

A major functional finding of this study is that rhSRGN significantly enhanced keratinocyte migration under hyperglycemic conditions, consistent with a chronic diabetic wound microenvironment. This effect was supported by elevated activation of migration-associated signaling markers, including p-p38 MAPK, p-Akt, p-Erk1/2, and TGFβ1. These pathways have been widely implicated in epithelial motility and wound closure dynamics[32]. Interestingly, rhSRGN exhibited an opposite effect under normoglycemic conditions, where keratinocyte migration and proliferation were reduced. A similar trend has been reported in fibroblasts treated with recombinant decorin, in which reduced cell proliferation was observed under normoglycemic conditions[33]. Moreover, previous studies linking serglycin to cancer cell migration were typically conducted under glucose concentrations comparable to the high-glucose conditions used here[34]. Therefore, the glucose-dependent response observed in this work suggests that serglycin bioactivity may be context-specific and influenced by metabolic state. This property may be particularly relevant for engineering wound therapeutics that are preferentially active in pathological environments.

Clinically, several wound-healing agents have been associated with increased cancer risk due to excessive stimulation of epithelial proliferation or induction of epithelial–mesenchymal transition under normal physiological conditions[35]. Because hyperglycemia restricts epithelial plasticity and impairs wound closure, diabetic wounds often require strong pro-migratory interventions[36]. In this context, rhSRGN may offer a potentially advantageous profile by enhancing migration under hyperglycemia while limiting excessive motility under normoglycemia. We previously reported that the therapeutic activity of

cobalt protoporphyrin, an inducer of heme oxygenase-1, in promoting wound closure is also influenced by glucose concentration in an *in vitro* model[37]. These findings suggest that the therapeutic efficacy of wound-healing agents may be modulated by glucose levels. However, this interpretation remains preliminary and requires validation in more physiologically representative systems.

Role of CD44 and Mechanistic Considerations

CD44 has been reported as a membrane receptor capable of interacting with serglycin and contributing to migratory signaling in cancer models[38]. In this study, CD44 silencing attenuated rhSRGN-mediated migration under hyperglycemia, accompanied by reduced expression of downstream migratory markers such as TGFβ1. These results are consistent with CD44 involvement in rhSRGN-associated signaling; however, it remains unclear whether rhSRGN directly activates CD44-dependent pathways or whether additional co-receptors and matrix interactions are required. Further mechanistic investigation will be necessary to define the receptor-level and intracellular signaling architecture.

CD44 silencing also reduced keratinocyte migration in both normoglycemic and hyperglycemic settings. Since CD44 has been linked to glucose metabolism and ATP generation pathways [39, 40], metabolic disruption may partially explain the reduced motility observed. Unexpectedly, rhSRGN enhanced migration in CD44-silenced cells under normoglycemia, suggesting the possibility of compensatory or CD44-independent mechanisms. These observations highlight the complexity of proteoglycan-mediated signaling in epithelial repair.

Taken together, our findings show that recombinant serglycin can be generated as a defined platelet-associated proteoglycan and selectively regulates keratinocyte migration in a glucose-dependent manner (Fig. 8). This work supports the broader strategy of using engineered platelet-derived components, rather than heterogeneous lysate preparations, as scalable and standardized biologics for diabetic wound repair.

Conclusions

Collectively, this study demonstrates that recombinant serglycin can be produced as a defined platelet-associated proteoglycan and can modulate keratinocyte migration in a glucose-dependent manner. These findings support the concept that engineered platelet-derived components, rather than heterogeneous lysate mixtures, may serve as scalable and standardized biologics for diabetic wound repair.

Several limitations of this study should be acknowledged. First, rhSRGN produced in HEK293T cells exhibited heterogeneous GAG decoration, including heparan sulfate chains that are not typically associated with platelet-derived serglycin. Future studies should incorporate glycoengineering strategies or alternative expression platforms to generate serglycin glycoforms that more closely resemble the native platelet phenotype. Second, the current work relies on an in vitro keratinocyte migration model. Although this system captures key aspects of re-epithelialization under hyperglycemic conditions,

validation in more complex wound models, including co-culture systems, engineered skin equivalents, and *in vivo* diabetic wound models.

Finally, the therapeutic translation of rhSRGN will depend on effective delivery strategies capable of achieving sustained localization within chronic wounds. Biomaterial-based approaches, such as hydrogel encapsulation or extracellular matrix–mimetic scaffolds, may enable controlled release and enhanced stability, supporting the development of rhSRGN as a next-generation biologic for regenerative wound engineering.

Declarations

Ethical Approval and Consent to Participate

Not applicable.

Consent for publication

Not applicable

Competing interests

The authors declare that they have no competing interests.

Funding

The authors would like to thank the financial support from National Science and Technology Council, Taiwan (109-2218-E-005 -004 -MY3).

Author Contribution

SWJ and BC designed the experiments and wrote the manuscript together. SWJ and BC analyzed and interpreted the data. SWJ and YNC conducted the experiments. YNC drew all the artwork presented in the manuscript. CCH and YTY provided feedback and suggestions on the manuscript.

Acknowledgement

Not Applicable.

Data Availability

All materials are available from the corresponding author.

References

1. Yen F-S, Yen Y-H, Hung Y-M, Wei JC-C, Tsai F-J, Hung Y-T, Lin H-J, Hwu C-M, Hsu C-C. Diabetic microvascular disease and risk of peripheral artery disease, foot Ulcer, leg infection, and amputation. Thromb Haemost 2025.
2. Su H-Y, Yang C-Y, Ou H-T, Chen S-G, Chen J-C, Ho H-J, Kuo S. Cost-effectiveness of novel macrophage-regulating treatment for wound healing in patients with diabetic foot ulcers from the Taiwan health care sector perspective. JAMA Netw open. 2023;6(1):e2250639–2250639.
3. Yadav JP, Singh AK, Grishina M, Pathak P, Verma A, Kumar V, Kumar P, Patel DK. Insights into the mechanisms of diabetic wounds: pathophysiology, molecular targets, and treatment strategies through conventional and alternative therapies. Inflammopharmacology. 2024;32(1):149–228.
4. Wang Y, Wu H, Pan Y, Xiao Y, Chen Y, Yang S, Wang J, Feng W, Hu C, Niu X. Innovations in hydrogel therapies for diabetic wound healing: bridging the gap between pathophysiology and clinical application. Burns Trauma. 2025;13:tkaf025.
5. Alhawari H, Jafar H, Al Soudi M, Ameereh LA, Fawaris M, Saleh M, Aladwan S, Younes N, Awidi A. Perilesional injections of human platelet lysate versus platelet poor plasma for the treatment of diabetic foot ulcers: A double-blinded prospective clinical trial. Int Wound J. 2023;20(8):3116–22.
6. Rodrigues RM, Valim VS, Berger M, da Silva AP, Fachel FN, Wilke II, da Silva WO, Santi L, da Silva MA, Amorin B. The proteomic and particle composition of human platelet lysate for cell therapy products. J Cell Biochem. 2022;123(9):1495–505.
7. Kolset SO, Pejler G. Serglycin: a structural and functional chameleon with wide impact on immune cells. J Immunol. 2011;187(10):4927–33.
8. Kolset S, Tveit H. Serglycin–structure and biology. Cell Mol Life Sci. 2008;65(7):1073–85.
9. Tellez-Gabriel M, Tekpli X, Reine TM, Hegge B, Nielsen SR, Chen M, Moi L, Normann LS, Busund L-TR, Calin GA. Serglycin is involved in TGF-β induced epithelial-mesenchymal transition and is highly expressed by immune cells in breast cancer tissue. Front Oncol. 2022;12:868868.
10. Lord MS, Cheng B, Tang F, Lyons JG, Rnjak-Kovacina J, Whitelock JM. Bioengineered human heparin with anticoagulant activity. Metab Eng. 2016;38:105–14.
11. Koupenova M, Livada AC, Morrell CN. Platelet and megakaryocyte roles in innate and adaptive immunity. Circul Res. 2022;130(2):288–308.
12. Schick BP, Ho H-CK, Brodbeck KC, Wrigley CW, Klimas J. Serglycin proteoglycan expression and synthesis in embryonic stem cells. Biochim et Biophys Acta (BBA)-Molecular Cell Res. 2003;1593(2–3):259–67.
13. Whitelock J. Purification of perlecan from endothelial cells. In: *Proteoglycan Protocols.* Springer; 2001: 27–34.

14. Varga CM, Hong K, Lauffenburger DA. Quantitative analysis of synthetic gene delivery vector design properties. Mol Ther. 2001;4(5):438–46.
15. Zheng W, Cai M-X, Peng H, Liu M, Liu X. Effect of glycosaminoglycans with different degrees of sulfation on chondrogenesis. Hua xi kou Qiang yi xue za zhi= Huaxi Kouqiang Yixue Zazhi= West China J Stomatology. 2023;41(4):395–404.
16. Lord MS, Whitelock JM. Recombinant production of proteoglycans and their bioactive domains. FEBS J. 2013;280(10):2490–510.
17. Adinata A, Hara T, Achyar AC, Nadanaka S, Suzuki Y, Kitagawa H, Igarashi M, Hirata K-I, Otake H, Emoto N. Chondroitin sulfate on leukocytes mediates thrombus resolution and organization: an in vivo imaging study. Am J Physiol Heart Circ Physiol. 2025;329(5):H1194–211.
18. Schütz A, Bernhard F, Berrow N, Buyel JF, Ferreira-da-Silva F, Haustraete J, Van den Heuvel J, Hoffmann J-E, De Marco A, Peleg Y. A concise guide to choosing suitable gene expression systems for recombinant protein production. STAR protocols. 2023;4(4):102572.
19. Moolsup F, Sukketsiri W, Sianglum W, Saetan J, Khumpirapang N, Tanasawet S. Sargassum plagiophyllum Ethanolic Extract Enhances Wound Healing by Modulating FAK/Src/Akt/p38 and Rac1 Signaling in Keratinocytes HaCaT Cells. Adv Pharmacol Pharm Sci. 2025;2025(1):7198281.
20. Guo J-Y, Chiu C-H, Wang M-J, Li F-A, Chen J-Y. Proteoglycan serglycin promotes non-small cell lung cancer cell migration through the interaction of its glycosaminoglycans with CD44. J Biomed Sci. 2020;27(1):1–18.
21. Stacey M, Mata S, Trengove N, Mather C. Randomised double-blind placebo controlled trial of topical autologous platelet lysate in venous ulcer healing. Eur J Vasc Endovasc Surg. 2000;20(3):296–301.
22. Chandra P, Faizan M, Porwal M, Sharma H, Sachan N. An overview and review of growth factors in wound healing: emerging trends and innovations. Curr Diabetes Rev. 2026;22(1):E15733998332692.
23. Lykins J, Becker IC, Camacho V, Alfar HR, Park J, Italiano J, Whiteheart SW. Serglycin controls megakaryocyte retention of platelet factor 4 and influences megakaryocyte fate in bone marrow. Blood Adv. 2025;9(1):15–28.
24. Reine TM, Vuong TT, Rutkovskiy A, Meen AJ, Vaage J, Jenssen TG, Kolset SO. Serglycin in quiescent and proliferating primary endothelial cells. PLoS ONE. 2015;10(12):e0145584.
25. Lord MS, Cheng B, Farrugia BL, McCarthy S, Whitelock JM. Platelet factor 4 binds to vascular proteoglycans and controls both growth factor activities and platelet activation. J Biol Chem. 2017;292(10):4054–63.
26. Chanzu H, Lykins J, Wigna-Kumar S, Joshi S, Pokrovskaya I, Storrie B, Pejler G, Wood JP, Whiteheart SW. Platelet α-granule cargo packaging and release are affected by the luminal proteoglycan, serglycin. J Thromb Haemost. 2021;19(4):1082–95.
27. Piszczatowski RT, Bülow HE, Steidl U. Heparan sulfates and heparan sulfate proteoglycans in hematopoiesis. Blood. 2024;143(25):2571–87.
28. Szekeres GP, Pagel K, Heiner Z. Analytical challenges of glycosaminoglycans at biological interfaces. Anal Bioanal Chem. 2022;414(1):85–93.

29. Fouché M, Willers C, Hamman S, Malherbe C, Steenekamp J. Wound healing effects of Aloe muth-muth: In vitro investigations using immortalized human keratinocytes (HaCaT). Biology. 2020;9(11):350.
30. Takatani-Nakase T, Matsui C, Maeda S, Kawahara S, Takahashi K. High glucose level promotes migration behavior of breast cancer cells through zinc and its transporters. PLoS ONE. 2014;9(2):e90136.
31. Nakai K, Kubota Y, Kosaka H. Inhibition of nuclear factor kappa B activation and inducible nitric oxide synthase transcription by prolonged exposure to high glucose in the human keratinocyte cell line HaCaT. Br J Dermatol. 2004;150(4):640–6.
32. Basu P, Martins-Green M. Signaling pathways associated with chronic wound progression: A systems biology approach. Antioxidants. 2022;11(8):1506.
33. Honardoust D, Varkey M, Hori K, Ding J, Shankowsky HA, Tredget EE. Small leucine-rich proteoglycans, decorin and fibromodulin, are reduced in postburn hypertrophic scar. Wound repair regeneration. 2011;19(3):368–78.
34. Korpetinou A, Skandalis SS, Moustakas A, Happonen KE, Tveit H, Prydz K, Labropoulou VT, Giannopoulou E, Kalofonos HP, Blom AM. Serglycin is implicated in the promotion of aggressive phenotype of breast cancer cells. PLoS ONE. 2013;8(10):e78157.
35. Sundaram GM, Quah S, Sampath P. Cancer: the dark side of wound healing. FEBS J. 2018;285(24):4516–34.
36. Tan MWY, Tan WR, Kong ZQ, Toh JH, Wee WKJ, Teo EML, Cheng HS, Wang X, Tan NS. High Glucose Restraint of Acetylcholine-Induced Keratinocyte Epithelial-Mesenchymal Transition Is Mitigated by p38 Inhibition. J Invest Dermatology. 2021;141(6):1438–49. e1439.
37. Fang P-H, Lai Y-Y, Chen C-L, Wang H-Y, Chang Y-N, Lin Y-C, Yan Y-T, Lai C-H, Cheng B. Cobalt protoporphyrin promotes human keratinocyte migration under hyperglycemic conditions. Mol Med. 2022;28(1):71.
38. Cao L, Luo FF, Huang HB, Huang TJ, Hu H, Zheng LS, Wang J, Peng LX, Qian CN, Huang BJ. The autoregulatory serglycin/CD44 axis drives stemness-like phenotypes in TNBC in a β-catenin-dependent manner. Clin translational Med 2021, 11(2).
39. Weng X, Maxwell-Warburton S, Hasib A, Ma L, Kang L. The membrane receptor CD44: novel insights into metabolism. Trends Endocrinol Metabolism. 2022;33:318–32.
40. Nam K, Oh S, Shin I. Ablation of CD44 induces glycolysis-to-oxidative phosphorylation transition via modulation of the c-Src–Akt–LKB1–AMPKα pathway. Biochem J. 2016;473(19):3013–30.

Figures

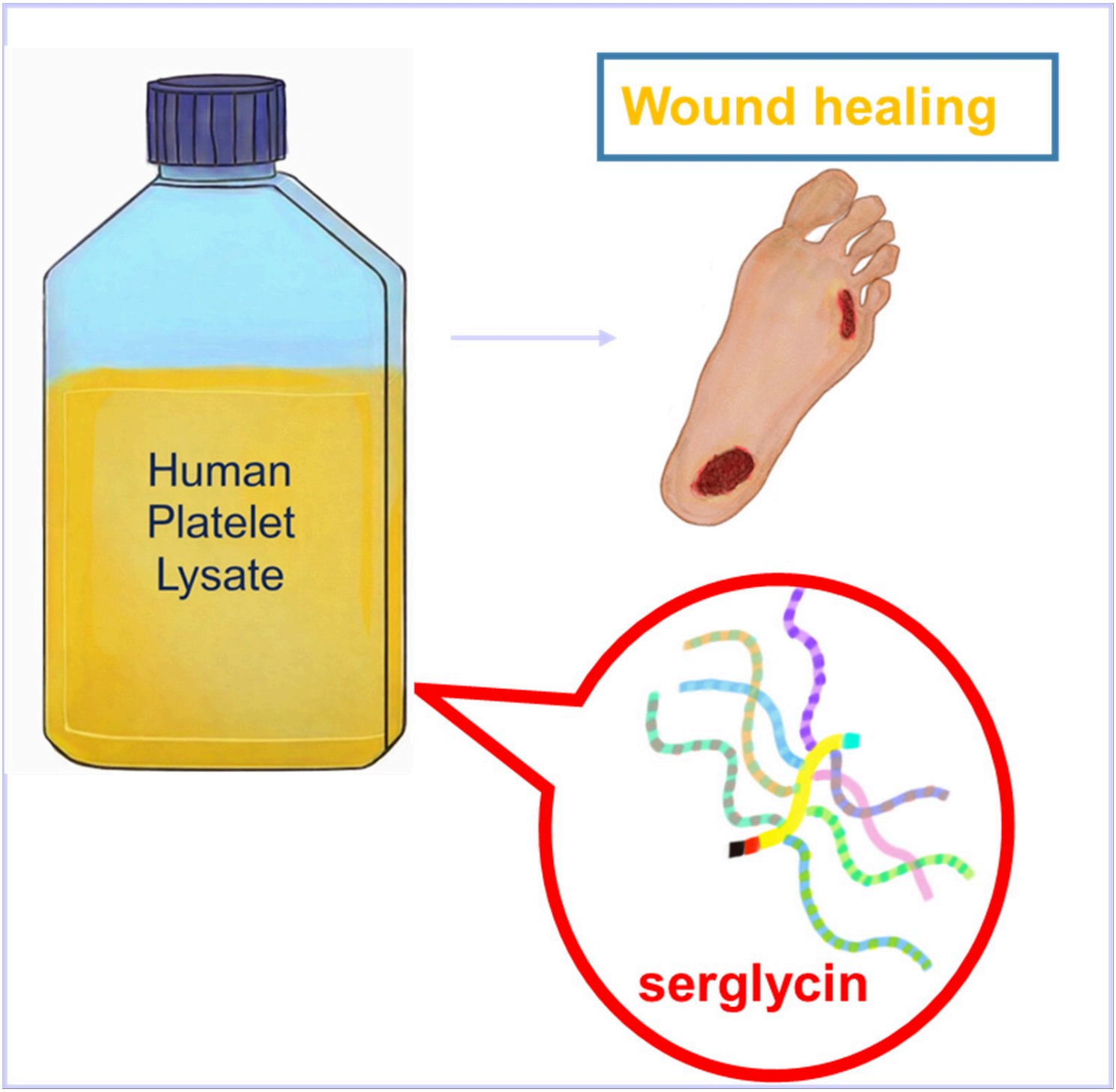


Figure 1

Schematic illustration of the study motivation. Human platelet lysate (hPL) is widely used in clinical applications, including wound healing. Although serglycin is a major component of hPL, its role in wound healing remains unclear.

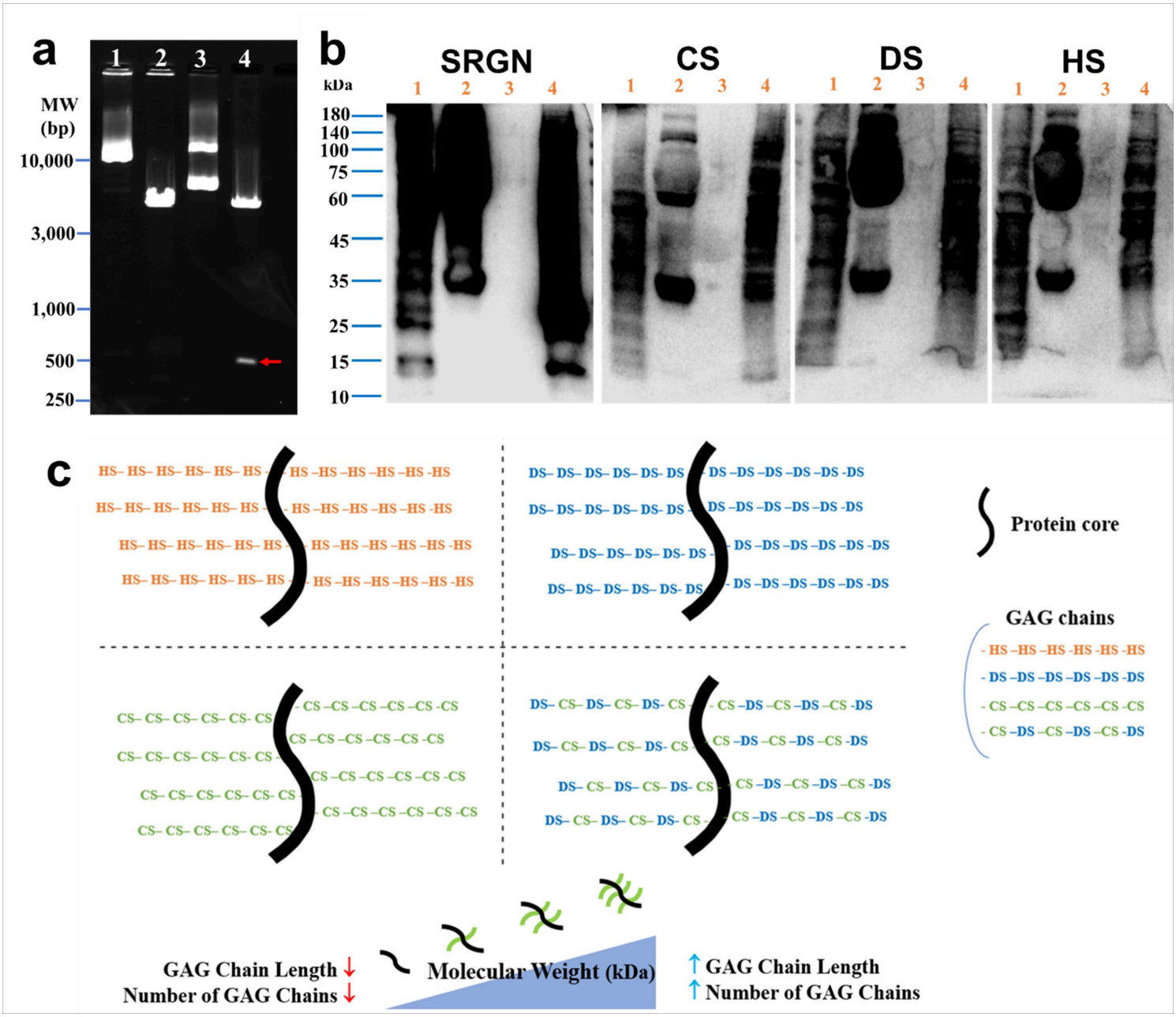


Figure 2

Analysis of the pcDNA4/SRGN-HisA recombinant vector and characterization of recombinantly expressed human serglycin (rhSRGN). (a) Restriction enzyme analysis of pcDNA4/HisA. The undigested pcDNA4/HisA vector is shown in lane 1, and the vector double-digested with *PmeI* and *BamHI* is shown in lane 2. Restriction analysis was also performed on the recombinant vector pcDNA4/SRGN-HisA using *PmeI* and *BamHI*. The double digest of pcDNA4/SRGN-HisA yielded a band at approximately 500 bp (lane 4, red arrow), in contrast to the undigested vector (lane 3). **(b)** Western blot analysis of THP-1 cell lysate (lane 1), hPL (lane 2), HEK293T cell lysate (lane 3), and purified rhSRGN (lane 4) using anti-human serglycin (SRGN),

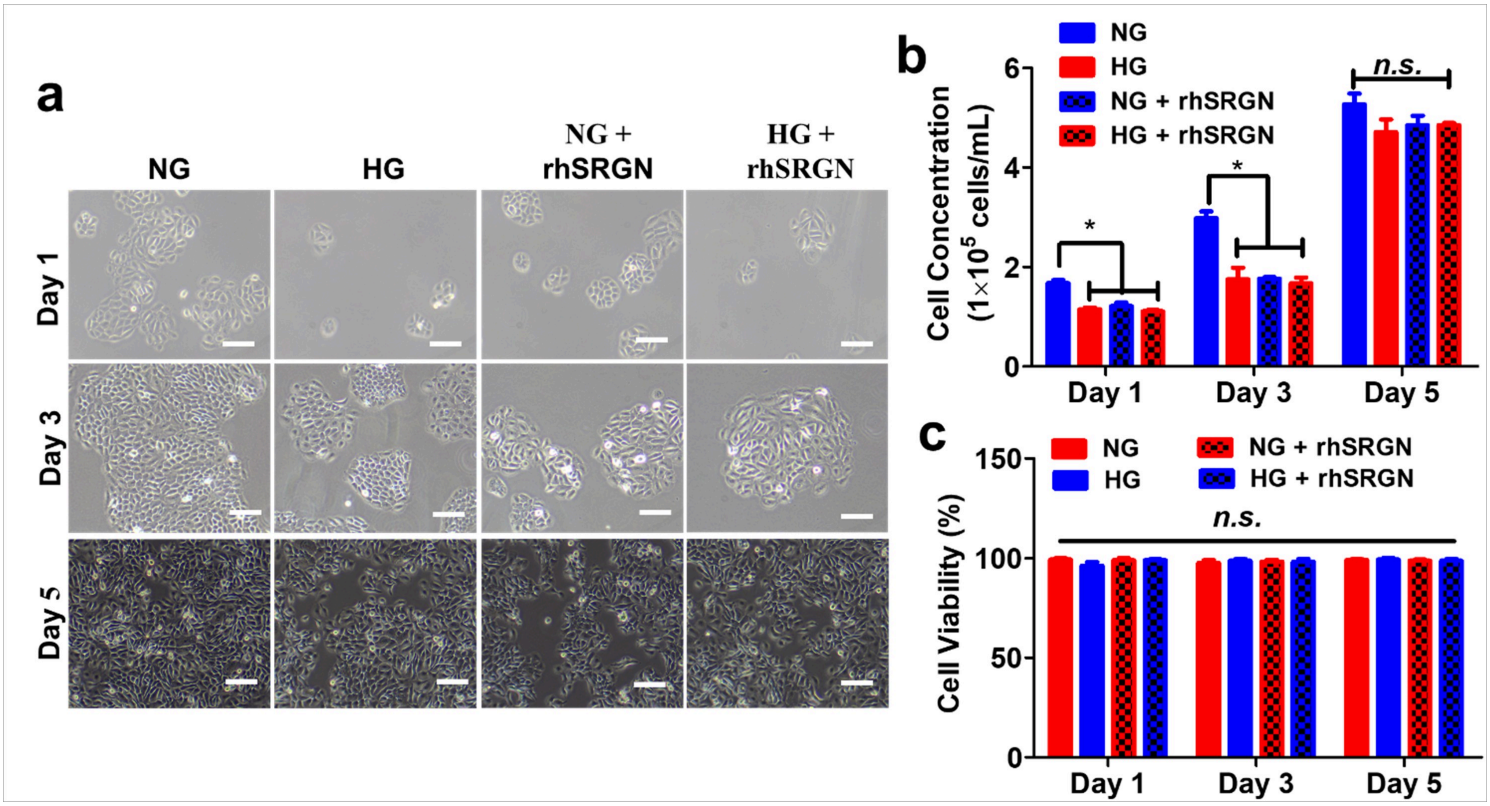


Figure 3

Effect of rhSRGN on HaCaT cell concentration under normoglycemic or hyperglycemic conditions.(**a**) HaCaT cells were cultured in medium containing either 5.5 mM glucose (normoglycemic, NG) or 25 mM glucose (hyperglycemic, HG). Results were compared with those from cultures supplemented with 10 ng/mL rhSRGN. Scale bar, 500 μm. (**b, c**) After imaging, cells from each group were trypsinized and subjected to cell counting (N = 3). *$P < 0.05$; *n.s.*, not significant.

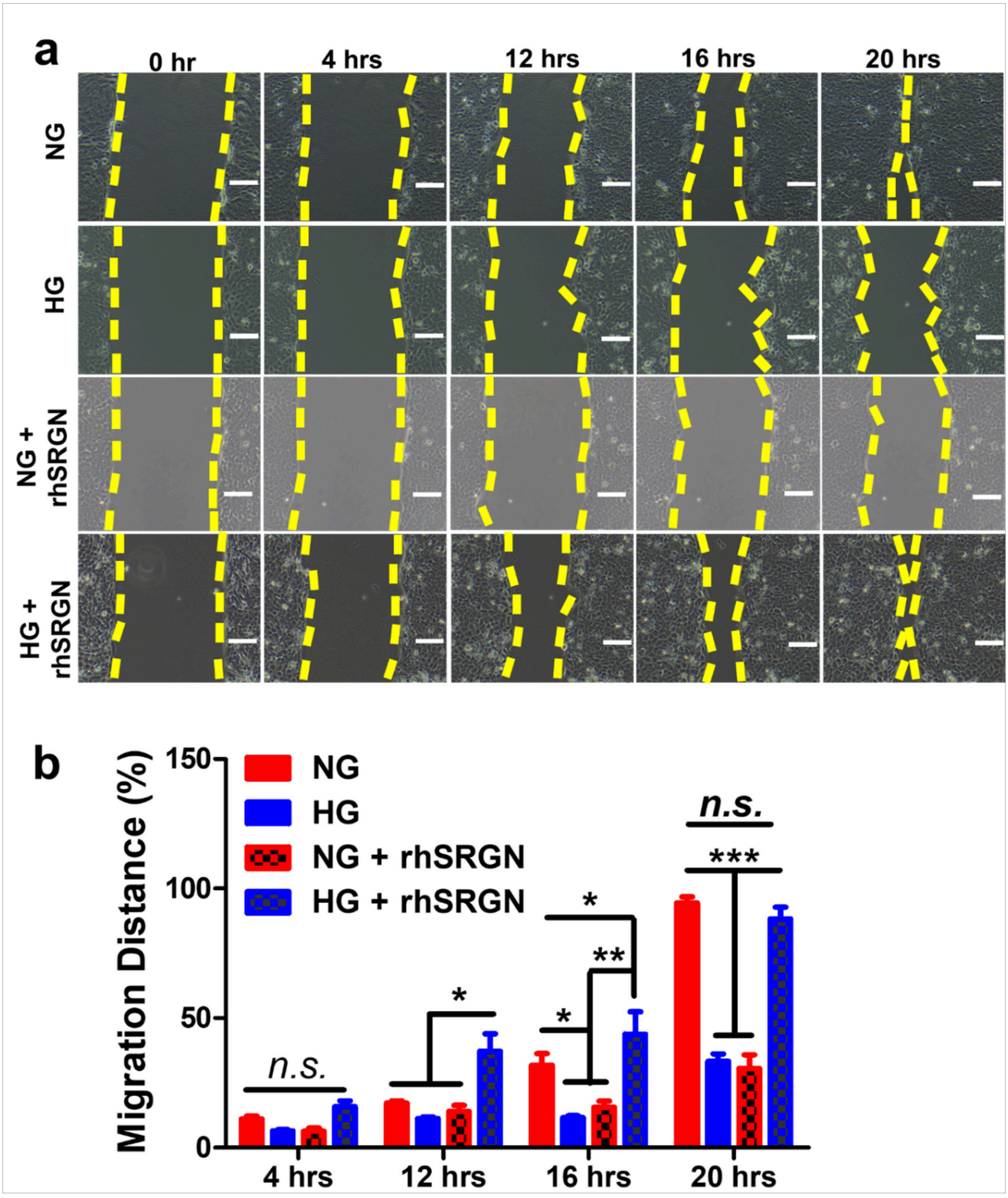


Figure 4

Effect of rhSRGN on HaCaT cell migration under normoglycemic or hyperglycemic conditions. (**a**) HaCaT cells were incubated in a Stage Top Incubator at 37°C for 20 h and imaged every 15 min. rhSRGN (10 ng/mL) was added to the designated groups. Scale bar, 100 μm. (**b**) Statistical analysis of the HaCaT cell migration rate under normoglycemic or hyperglycemic conditions. N = 3; *$P < 0.05$; **$P < 0.01$; ***$P < 0.001$; *n.s.*, not significant.

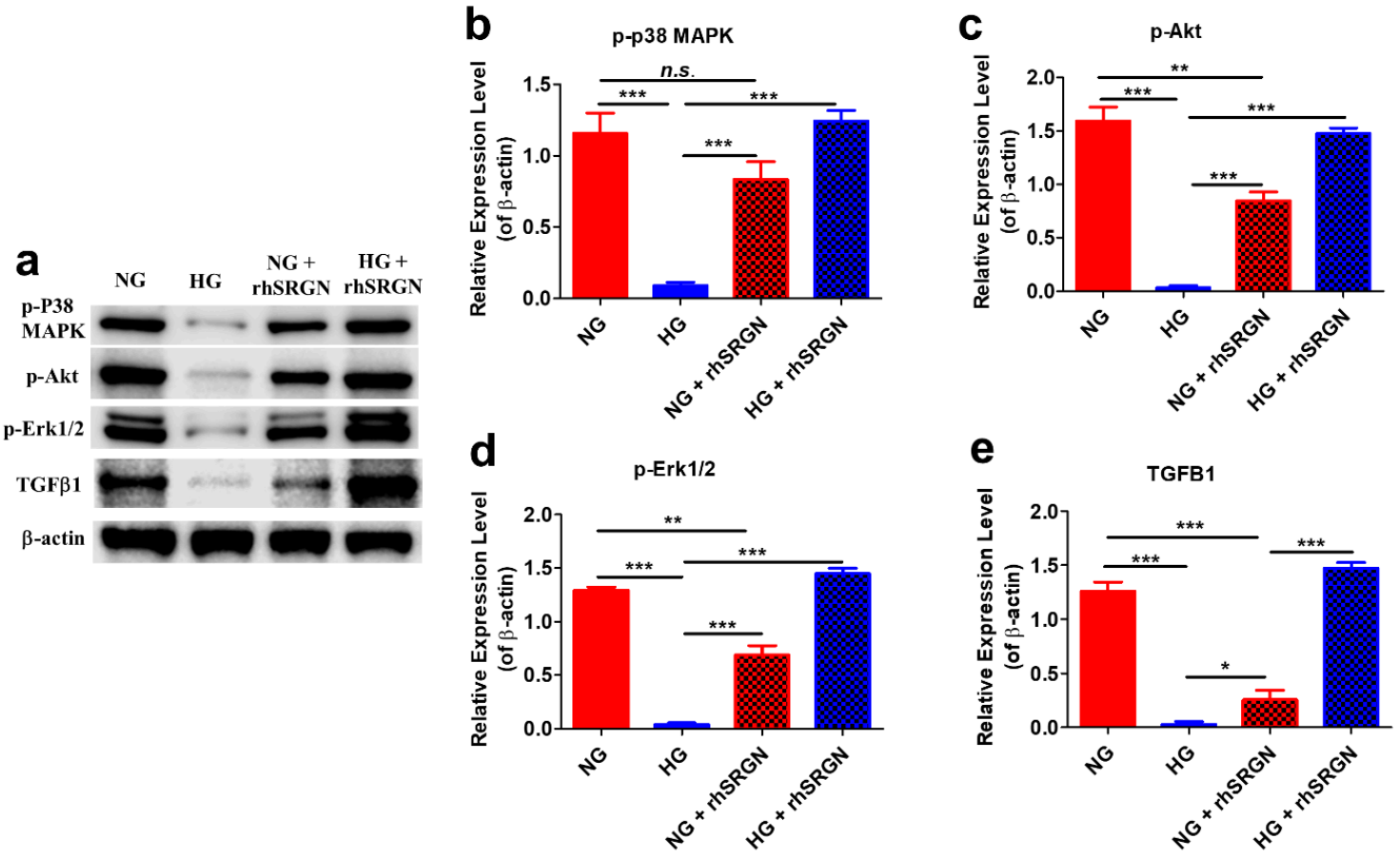


Figure 5

Western blotting analysis of migratory protein expressions in HaCaT that underwent migration in the absence or presence of rhSRGN. (**a**) After 20 h of imaging, cell lysates were harvested from cells in all sample groups and subjected to Western blotting analysis. (**b-e**) The statistical analysis of the protein expressions in HaCaT that underwent migration under normoglycemia or hyperglycemia, with or without rhSRGN (10 ng/mL)**.** N=3; *, *P*<0.05; **, *P*<0.01; ***, *P*<0.001; *n.s.*, not significant.

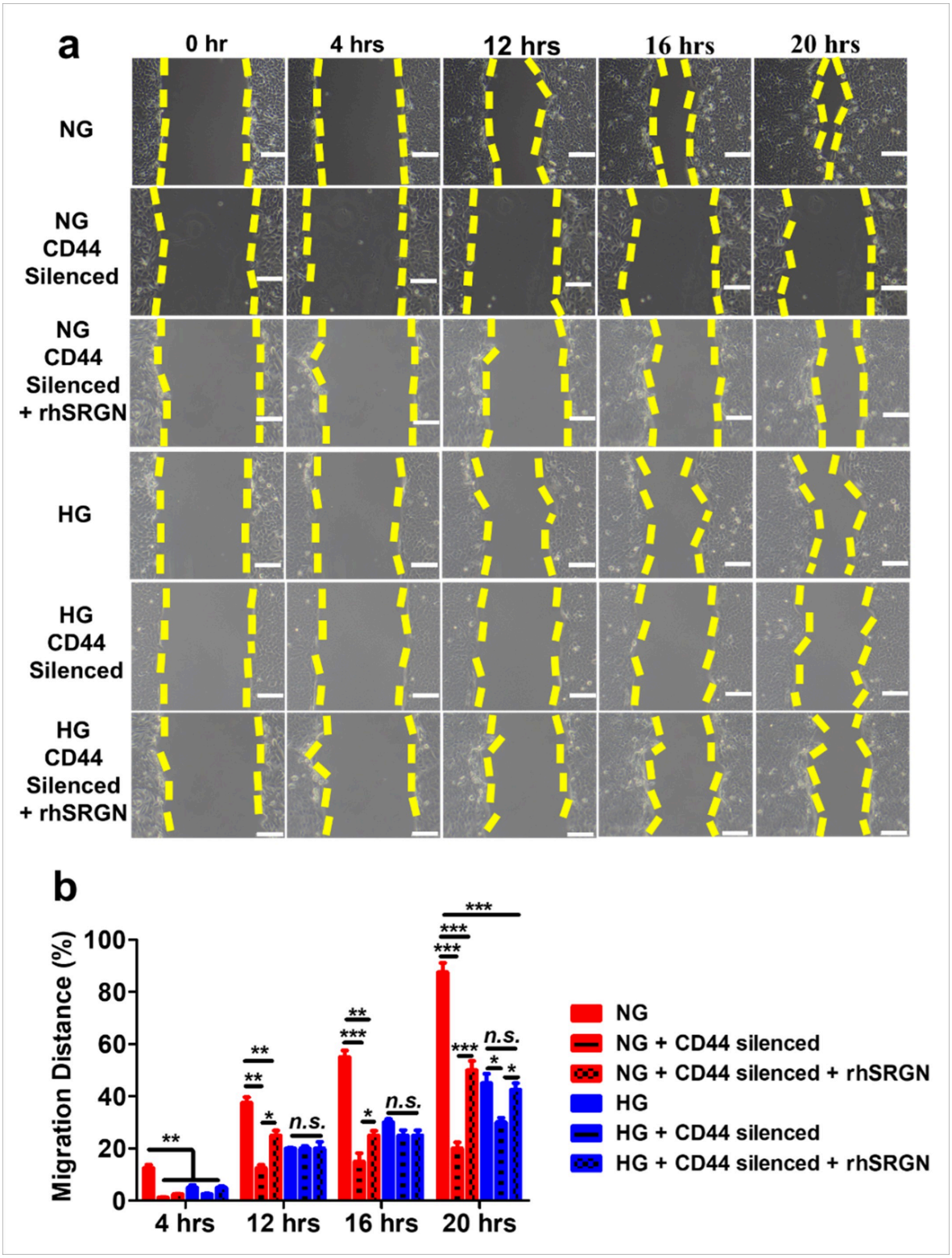


Figure 6

Time-lapse images of CD44 siRNA-treated HaCaT in NG or HG media. (a) HaCaT cells that received negative control siRNA (NG or HG) or CD44 siRNA (NG or HG CD44 Silenced) underwent cell migration in NG or HG media, and the results were compared to the cells that received 10 ng/mL rhSRGN (NG or HG CD44 + rhSRGN). Scale bar, 100 mm. (**b**) Statistical analysis of the migration rate of HaCaT and CD44

siRNA-treated HaCaT in either NG or HG media, with or without the addition of rhSRGN. N =3; *, *P*<0.05; **, *P*<0.01; ***, *P*<0.001; *n.s.*, not significant.

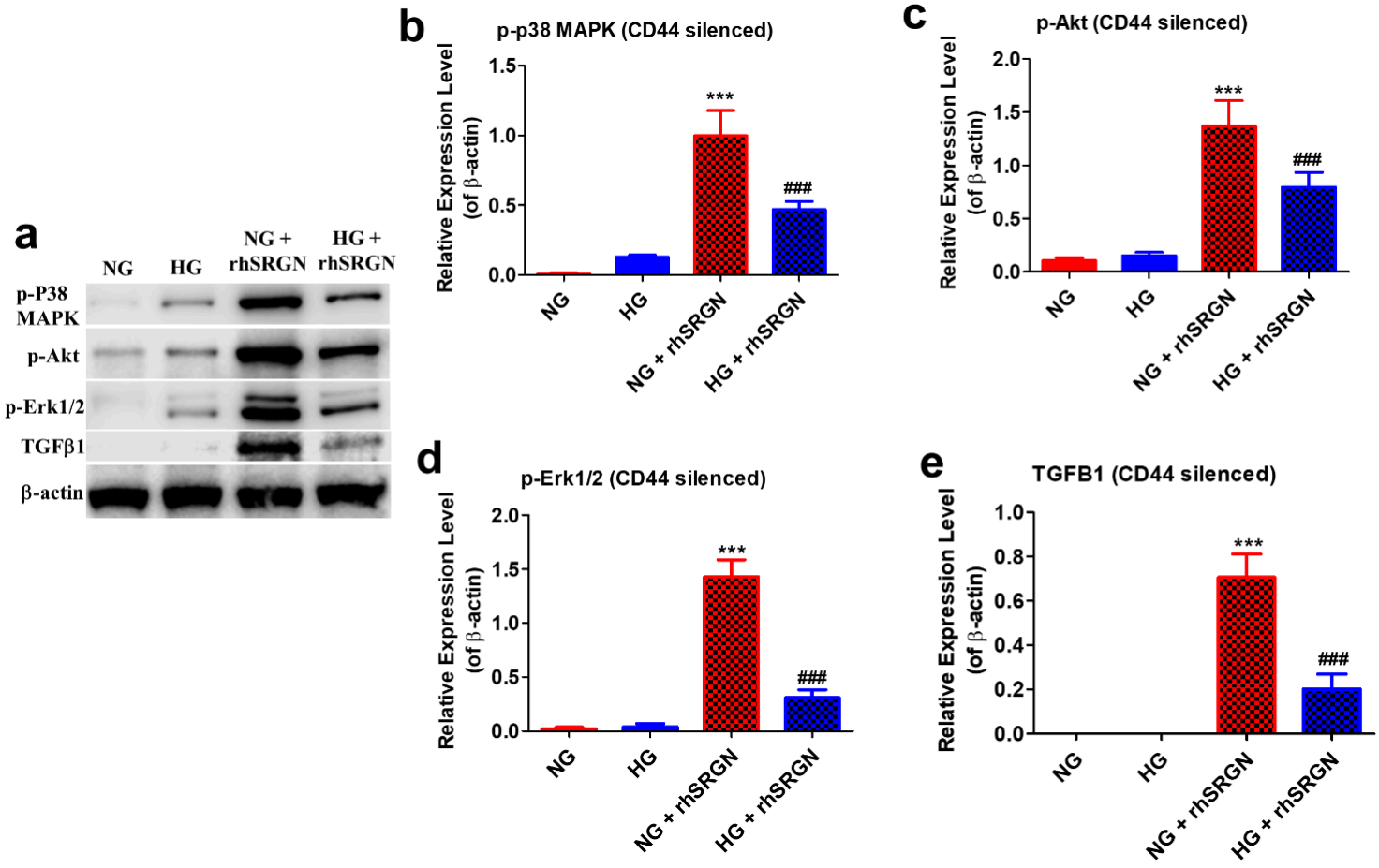


Figure 7

Western blot analysis of migratory protein expression in CD44-silenced HaCaT cells that underwent migration in the absence or presence of rhSRGN. (**a**) After 20 h of imaging, cell lysates were harvested from all the CD44-silenced cells in each sample with or without rhSRGN (10 ng/mL) and subjected to Western blotting analysis. (**b-e**) The statistical analysis of protein expression in each analyzed group. N=3; ***, *P*<0.001 vs NG; ###, *P*<0.001 vs HG.

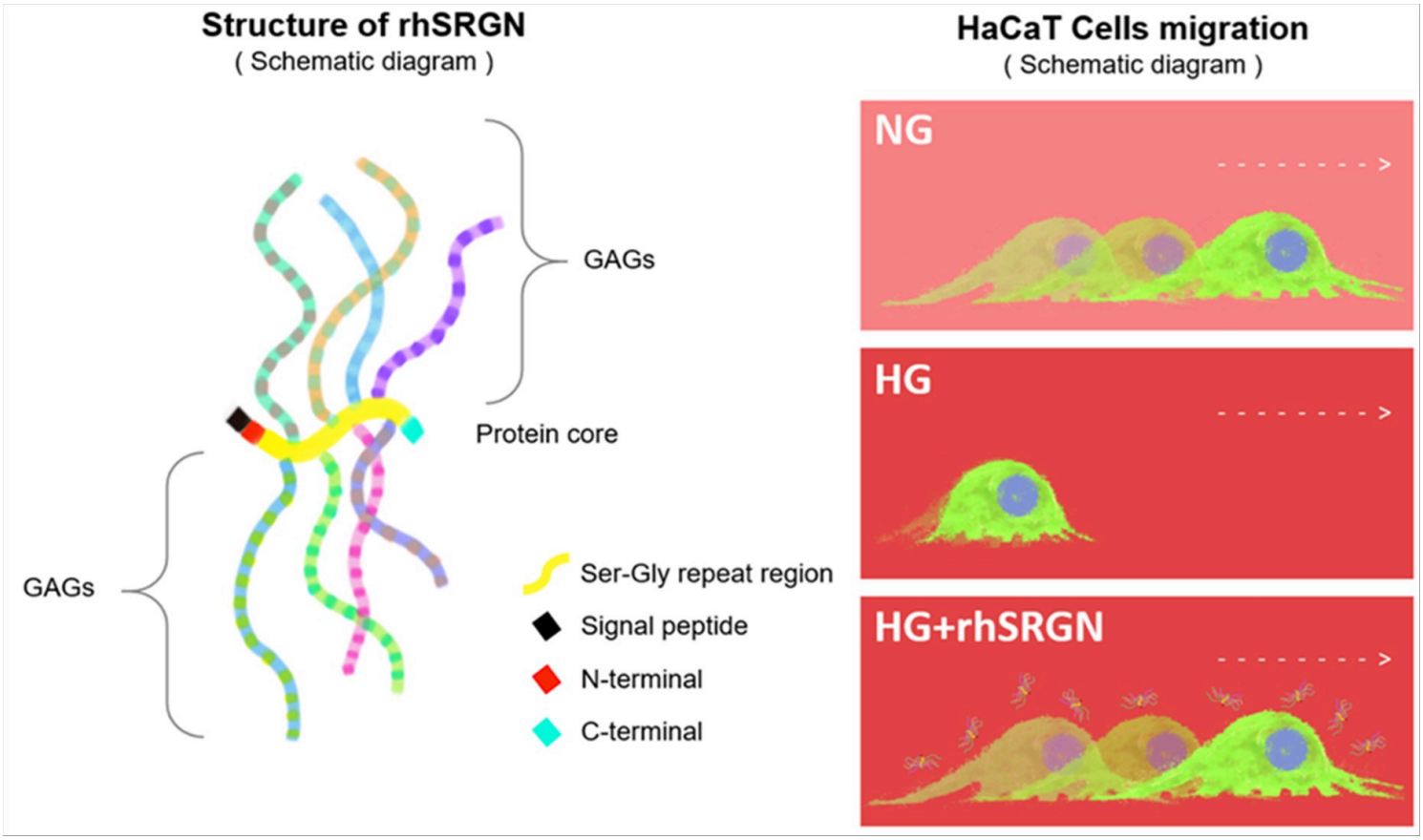


Figure 8

The schematic diagram summarizes the main findings of the present study. Recombinant human serglycin (rhSRGN) was successfully expressed and demonstrated to have CS, DS, and HS as the GAG chains. The presence of the rhSRGN could significantly enhance HaCaT migration under hyperglycemia.

Supplementary Files

This is a list of supplementary files associated with this preprint. Click to download.

- rhSRGNwoundhealingJBESupplementaryV02.docx